Short Communication

The Precrystalline Cytoplasmic Granules of Alveolar Soft Part Sarcoma Contain Monocarboxylate Transporter 1 and CD147

Marc Ladanyi,* Cristina R. Antonescu,*
Marija Drobnjak,* Ann Baren,* Man Yee Lui,*
David W. Golde,[†] and Carlos Cordon-Cardo*

From the Departments of Pathology* and Medicine,[†] Memorial Sloan-Kettering Cancer Center, New York, New York

Alveolar soft part sarcoma (ASPS) is an unusual tumor of young adults with the characteristic presence on ultrastructural analysis of rhomboid or rectangular cytoplasmic crystals. These membrane-bound crystals are known to form within specific PAS-diastase-resistant electron-dense cytoplasmic granules. The composition of these crystals and the dense granules from which they are derived has remained elusive. After the detection of strong discrete granular cytoplasmic immunoreactivity in ASPS for monocarboxylate transporter 1 (MCT1) in the course of a broad immunohistochemical characterization of an MCT1 antibody, we studied the expression of MCT1 and its interacting partner, CD147, in a panel of 10 ASPS cases using appropriate antibodies. MCT1 is one of a family of widely expressed proton-linked transporters for monocarboxylates such as lactate and pyruvate. In all normal and neoplastic tissues studied to date, MCT1 immunoreactivity is limited to the cell surface. We find that the periodic acid-Schiff-diastase-resistant cytoplasmic granules of ASPS are strongly immunoreactive for MCT1 and CD147. Specifically, intense cytoplasmic granular positivity for MCT1 and CD147 was found in 7 of 10 and 8 of 10 ASPSs, respectively. Ultrastructural immunohistochemistry with immunogold labeling confirmed that the MCT1 immunoreactivity localized to the cytoplasmic electron-dense granules in ASPS. Western blot analysis of several ASPS cases confirmed that the protein reactive with the MCT1 antibody and that reactive with the CD147 antibody both migrated at the size expected for MCT1 and CD147, respectively. Thus, ASPS cells seem to accumulate MCT1-CD147 complexes in the specific cytoplasmic granules known to undergo crystallization. The possible basis for the overproduction or impaired surface localization of these proteins in ASPS remains unclear. *(Am J Pathol 2002, 160:1215–1221)*

Alveolar soft part sarcoma (ASPS) is an unusual tumor with a highly characteristic histopathology and ultrastructure, controversial histogenesis, and often enigmatic clinical behavior.[1–3] ASPS was first recognized and described in 1952.[4] Most cases of ASPS occur in the second and third decade of life, with a slight female predilection.[1,3] It usually involves the muscle and deep soft tissues of the extremities (classically the thigh), but has also been reported in tissues where skeletal muscle is absent. Its cell of origin or lineage has remained unclear.[2] ASPS is characterized cytogenetically by a recurrent chromosomal translocation resulting in a consistent der(17)t(X;17)(p11;q25)[5,6] that has recently been shown to result in the fusion of the *TFE3* transcription factor gene (from Xp11) with a novel gene at 17q25, named *ASPL*.[7] *ASPL* encodes a ubiquitously expressed cytoplasmic protein whose physiological role remains obscure.[7] ASPL-TFE3 can function as a transcription factor (MY Lui, M Ladanyi, unpublished data) but the target genes that it may aberrantly regulate are presently unknown.

Cytoplasmic granules, sometimes with a crystalline appearance, are a classical histological feature of ASPS, first noted by Masson in the 1950's.[8] The typical ASPS crystals seem to form within these cytoplasmic dense granules that are periodic acid-Schiff (PAS)-positive and diastase-resistant (excluding glycogen as their content). The earliest histochemical and ultrastructural analysis of ASPS by Shipkey and colleagues[8] indicated that these crystals and dense granules contained protein and polysaccharides, were often rhomboid, rectangular, or polygonal in overall shape and membrane-bound, and the

Table 1. Results of MCT1 and CD147 Immunostaining

ASPS case*	Age, sex	Primary site	*ASPL-TFE3* fusion type	PASD granules	MCT1 immunostaining			CD147 immunostaining		
					Membrane staining	Cytoplasmic staining		Membrane staining	Cytoplasmic staining	
						Diffuse	Discrete granules		Diffuse	Discrete granules
1	19 F	Thigh	1	++	++	−	+++	++	+	++
2	36 F	Axilla	2	++	+	−	+++	−	+	++
3	31 F	Thigh	1	+	+f	−	−	+f	+	+
4	38 M	Arm	2	+++	+f	+	+++	−	+	++
5	29 F	Thigh	1	++	+	+	+ rare	++	+	+
7	40 F	Thigh	1	++	+f	−	−	+f	−	−
14	36 F	Thigh	1	++	+	−	++	++	+	+
15	41 M	Shoulder	†	−	+f	++	−	−	+	+
16	36 F	Thigh	n.a.	+++	++	+	+++	+	++	++
17	21 F	Thigh	‡	+	++	−	+ rare	−	−	−

+, few; ++, moderate; +++, many; f, focal; n.a., not available.

*Unique case numbers from serial collection of ASPS samples.

†*TFE3* genomic rearrangement demonstrated by Southern blot analysis (see text). No RNA available for reverse-transcriptase-polymerase chain reaction.

‡Cytogenetic evidence of t(X;17) (see text). No RNA available for reverse-transcriptase-polymerase chain reaction.

constituent fibers in fully developed crystals had a periodicity of 10 nm and a diameter of 4.5 to 5.0 nm. It should be noted that the classic cytoplasmic crystals are only found in approximately half of ASPSs, whereas the remaining cases instead show mainly the characteristic cytoplasmic dense granules consisting of fine filamentous material, sometimes with early crystallization.[9–11]

In characterizing a polyclonal antibody to monocarboxylate transporter 1 (MCT1), intense cytoplasmic reactivity was noted in ASPS but not in other tumors. In all other normal and neoplastic tissues, MCT1 immunoreactivity was limited to the cell surface (M Drobnjak, C Cordon-Cardo, unpublished data). Prompted by this initial observation, we performed further light and ultrastructural immunohistochemistry (IHC), and Western blot analyses of MCT1 and its interacting partner CD147. The results reported here suggest that ASPS cells specifically accumulate MCT1-CD147 complexes in their cytoplasm, presumably leading to their crystallization. The significance of these findings to the biology of ASPS or to its lineage of origin is unclear.

Materials and Methods

ASPS Case Material

We studied 10 cases of ASPS, selected solely on the basis of available paraffin-embedded tumor material, including 8 from Memorial Sloan-Kettering Cancer Center, and one each from the University of Nebraska Medical Center (Omaha, NE) and the Center for Human Genetics, University of Leuven (Leuven, Belgium). Six cases were included in a previous study (cases ASPS-1 to 5, and ASPS-7).[7] The presence of the *ASPL-TFE3* fusion was documented by reverse transcriptase-polymerase chain reaction in seven cases (cases ASPS-1 to 5, ASPS-7, and ASPS-12), performed as described previously.[7] The remaining three cases did not have material available for reverse transcriptase-polymerase chain reaction testing,

but two cases had other evidence of the *ASPL-TFE3* rearrangement. Case ASPS-15 showed a *TFE3* genomic rearrangement by Southern blotting (not shown), performed using a *TFE3* intron 3 probe as previously described.[7] Case ASPS-17 was originally reported to contain a cytogenetic add(17)(q25),[12] but its karyotype has been revised as follows: 45,XX,del(1)(p11),der(9)t(9;15)(p11;q11), der(17)t(X;17)(p11;q25),-22.[7] Basic clinicopathological data are summarized in Table 1.

IHC Analysis

A polyclonal rabbit antibody to MCT1 was generated as follows. A peptide representing the 24-carboxyl amino acids of human MCT1 (VTKTAESPDQKDTEGGP-KEEESPV) was synthesized with an amino-terminal cysteine. The peptide was conjugated to KLH and rabbits were immunized. The rabbit antiserum was affinity purified and used at a dilution of 1:20,000. For CD147, a mouse monoclonal antibody reactive to human CD147 (clone HIM6; Research Diagnostics Inc, Flanders, NJ) was used at a concentration of 5 μg/ml. Staining was performed on 5-μm formalin-fixed, deparaffinized tissue sections using the avidin-biotin-peroxidase method with antigen retrieval. Briefly, after deparaffinization slides were quenched with 0.1% H_2O_2 to reduce endogenous peroxidase staining, washed in phosphate-buffered saline (PBS), and heated in the presence of 0.01 mol/L citric acid, pH 6.0, in a microwave oven for 15 minutes. After cooling to room temperature, slides were washed and incubated with adequate blocking sera (10% normal goat serum and 10% normal horse serum, respectively) for 30 minutes. Primary antibodies were then applied and left for overnight incubation at 4°C. After extensive washing with PBS, anti-rabbit and anti-mouse IgGs were used as secondary antibodies at a dilution of 1:500, followed by avidin-biotin complex at 1:25 dilution. Finally, diaminobenzidine was used as a chromogen with H_2O_2 as a

MCT1   CD147
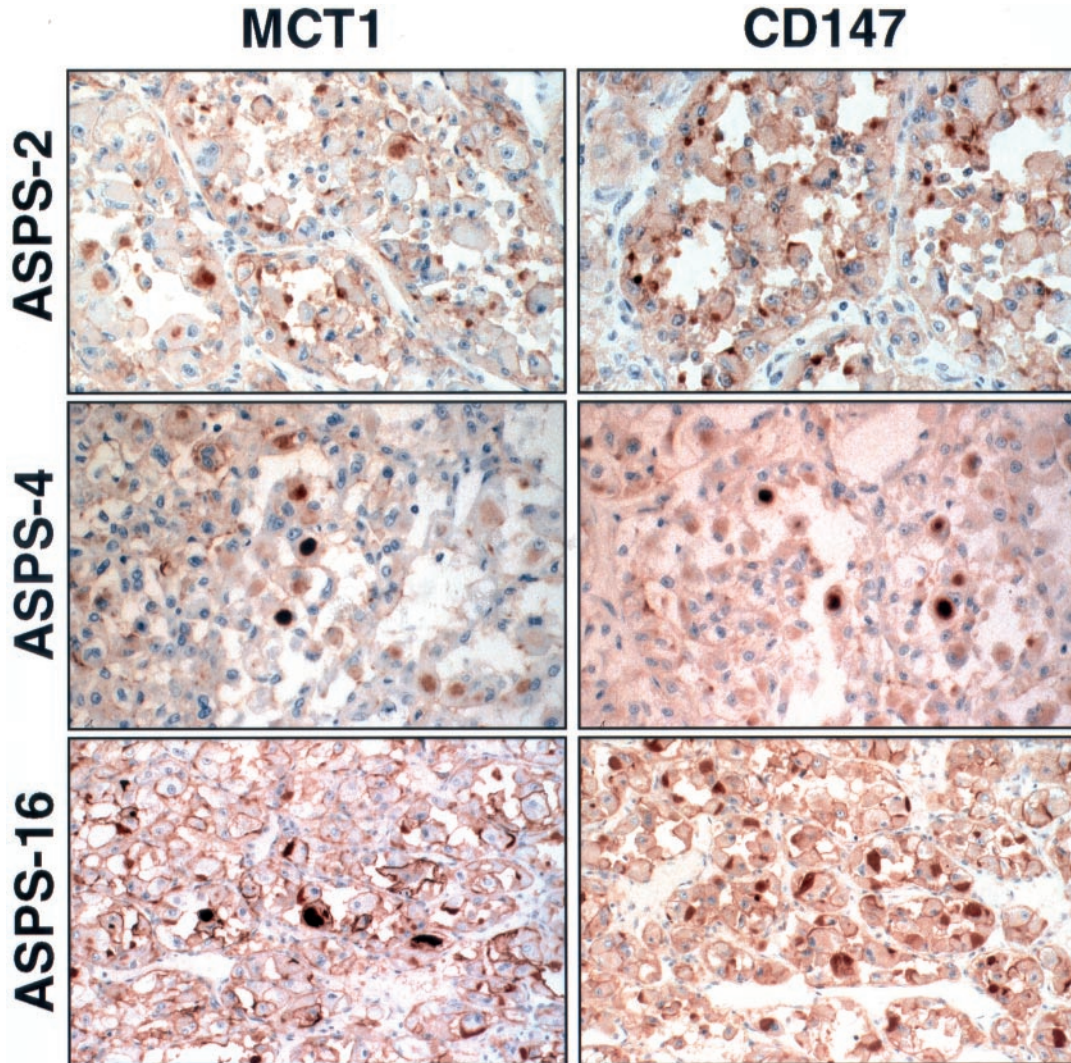
Figure 1. Coincident pattern of MCT1 and CD147 cytoplasmic immunoreactivity in ASPS. Paired MCT1 and CD147 immunostains are illustrated in three ASPS cases. Note that the size and shape of MCT1- and CD147-immunoreactive cytoplasmic granules are essentially identical in each case. Paired fields are shown at the same magnification for cases ASPS-4 and ASPS-16. For case ASPS-2, the magnification of the CD147 immunostain is slightly lower than the corresponding MCT1.
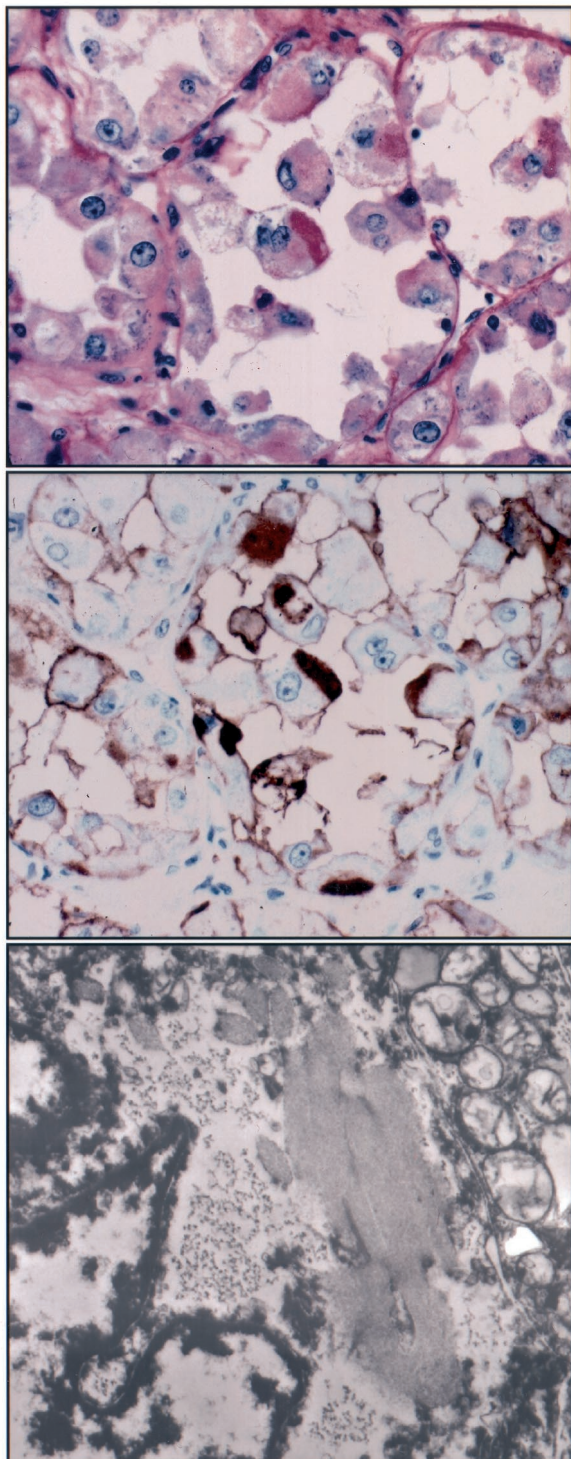
substrate and slides were counterstained with light hematoxylin.

Ultrastructural IHC Analysis

Representative fresh tumor tissue was fixed in EMS fixative (3% glutaraldehyde and 3% paraformaldehyde in 0.1 mol/L Millonig's phosphate buffer, pH 7.4 (Electron Microscopy Sciences, Fort Washington, PA) and held in phosphate buffer until embedded in LR White Resin (Ted Pella, Inc., Redding, CA) using standard procedures. In each case, thick sections were cut (1 μm) and stained with toluidine blue to select suitable tissue for analysis. Thin sections (90 to 100 nm) were cut and placed on uncoated 300 mesh nickel grids (Ted Pella, Inc). Grids were then pretreated using 10% Na-metaperiodate for 1 hour at room temperature, and washed in distilled water for 5 minutes, followed by soaking in 0.01 mol/L of sodium citrate, pH 6.0, that had been microwaved to 90°C. The

grids in solution were kept on a hot plate for 10 minutes and allowed to cool for 15 minutes. After rinsing with distilled water, the grids were then placed in a blocking solution of 2% bovine serum albumin/PBS for 10 minutes at room temperature and incubated in the primary antibody [MCT1 (1:500; 1:1000) diluted with 20 mmol/L Tris sodium buffer, pH 8.25] overnight at 4°C. The grids were then rinsed with 20 mmol/L of Tris sodium buffer and soaked for 5 minutes in the same solution. A goat anti-rabbit IgG (1:1500 with 20 mmol/L of Tris sodium buffer) was used for the rabbit polyclonal MCT1 antibody for 30 minutes at room temperature. The grids were then again rinsed with 20 mmol/L of Tris sodium buffer and soaked for 5 minutes in the same solution. A 10-nm protein A gold conjugate (BB International, Cardiff, UK) diluted 1:10 with 20 mmol/L of Tris sodium buffer was then applied to grids for 2 hours at room temperature, followed by two rinses with PBS. The grids were then stained with uranyl acetate for 10 minutes and lead citrate for 10 minutes.

Western Blot Analysis

Cells were washed twice in PBS and cell pellets were resuspended with 1× lysis buffer with phenylmethyl sulfonyl fluoride and 2 μg/ml leupeptin proteinase inhibitor, vortexed immediately, and placed on ice for 30 minutes. Cell debris was spun down and the supernatant was recovered and an equal volume of 2× sodium dodecyl sulfate gel-loading buffer was added to it. The cell lysate was boiled for 10 minutes and an aliquot loaded on an 10% sodium dodecyl sulfate-polyacrylamide gel. The electrophoresed proteins were transferred to a nitrocellulose membrane, and the membrane was covered with blocking solution and incubated at 4°C overnight. The blot was probed with MCT1 antibody diluted 1:1000 or with CD147 antibody diluted 1:500, followed, respectively, by secondary anti-rabbit or anti-mouse antibody conjugated to horseradish peroxide using the ECL detection system (Amersham Pharmacia Biotech, Piscataway, NJ) and the membrane was applied to X-ray film.

Results

Immunohistochemical Analysis

All 10 ASPS cases showed membrane immunoreactivity for MCT1, ranging from intense diffuse labeling to focal moderate labeling. In addition to this pattern of MCT1 immunostaining, which is similar to that observed in other tissues and tumors, 7 of 10 cases also showed intensely staining cytoplasmic spherical globules or polygonal inclusions that were widespread in four cases and less frequent in three cases (Figure 1). Finally, four cases displayed weak to moderate diffuse cytoplasmic MCT1 staining in three cases in addition to the above intensely staining cytoplasmic inclusions. IHC for CD147, which functions as an MCT1 chaperone protein, revealed a strikingly coincident pattern of cytoplasmic staining. Thus, in cases with spherical or polygonal cytoplasmic inclusions immunoreactive for MCT1, cytoplasmic inclusions of the same shape, frequency, and distribution were decorated by CD147 immunostaining in each case (Figure 1). Most ASPSs showed diffuse cytoplasmic reactivity for CD147, but cell membrane positivity was less prominent than for MCT1. To correlate the MCT1/CD147 immunoreactive inclusions with the characteristic PAS-positive diastase-resistant cytoplasmic granules of ASPS, the same cases were studied with the latter histochemical stain. Again, there was a strong concordance in the shape, frequency, and distribution of the latter histochemically defined granules with the former inclusions revealed by immunostaining. In one case, the MCT1 IHC and the PAS stain with diastase digestion were done on serial sections, establishing the identity of the cytoplasmic inclusions demonstrated by these two methods (Figure 2).

Ultrastructural IHC

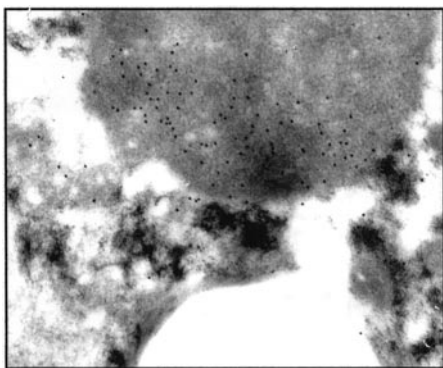Conventional ultrastructural observations on the crystals and granules in nine of our cases are summarized in

Figure 2. Cytoplasmic MCT1 immunoreactivity in ASPS corresponds to the characteristic PAS-positive diastase-resistant granules associated with crystal formation. **Top:** PAS-diastase-stained section of case ASPS-16 shows PAS-positive diastase-resistant angular dark-pink cytoplasmic granules in several cells, notably in the tumor cell at the center of the field. The typical histology of ASPS is apparent, consisting of well-defined nests of cells with abundant pink cytoplasm with a loss of central cohesion producing a pseudoalveolar appearance. **Middle:** MCT1 IHC of serial section of same case (ASPS-16) gives intense immunostaining of the same angular cytoplasmic granule, along with staining at the cell surface. **Bottom:** Ultrastructural examination of partially formed cytoplasmic crystals (lacking distinct periodicity) in another cell from this case (ASPS-16) shows an angular and linear arrangement corresponding in shape and orientation to the specific cytoplasmic granules highlighted by the PAS-diastase stain and the MCT1 IHC (original magnifications, ×10,400).

Table 2. Ultrastructural Appearance of Crystals and Granules

ASPS case	Characteristic crystals	Dense granules
1	Many complex/geometric shape crystals, mostly with homogeneous/granular content, uneven and only focal lattice/internal structure; rare classic rhomboid-shaped with 10-nm periodicity	Rare
2	Numerous very large complex/geometric shape crystals, with uneven lattice/internal structure; few long classic rhomboid-shaped crystals with 10-nm periodicity	Frequent
3	Moderate number of complex crystals with uneven lattice; rare rhomboid-shaped crystals with classic 10-nm fiber periodicity	Frequent, some with early crystallization
4	Absent	Frequent
5	Few rhomboid-shaped crystals with homogenous/granular content; no well-formed lattice	Frequent
7	Rare crystals with well-formed lattice	Rare
15	Numerous long classic rhomboid-shaped crystals with 10-nm fiber periodicity; few more complex crystals with uneven lattice	Frequent
16	Long rhomboid and also complex-geometric-type crystals mostly with homogenous/granular content; no well-formed lattice	Frequent
17	Rare classic rhomboid crystals with 10-nm periodicity; no large complex crystals	Very rare

Table 2. Material was available for ultrastructural IHC in cases ASPS-1, ASPS-2, and ASPS-14. In all three cases, ultrastructural IHC with the MCT1 antibody resulted in deposition of gold particles on the cytoplasmic dense granules (Figure 3), and on mitochondria (not shown). The presence of MCT1 in mitochondria is well described.[13]

Western Blot Analysis

To confirm that the epitopes in ASPS that are immunoreactive with the anti-MCT1 and anti-CD147 antibodies indeed belong to MCT1 and CD147, respectively, we performed Western blot analysis on four cases with available material. All four cases tested showed bands of appropriate size with both antibodies, namely 43 kd for MCT1 and 42 kd for CD147[14] (Figure 4). There was no obvious relationship between the levels of MCT1 and CD147 in these four cases. These results confirm that these ASPS cases contain MCT1 and CD147, but given the widespread normal expression of these proteins, they do not in themselves indicate the immunoreactive material in the

Western blots corresponds to the cytoplasmic granules decorated by immunostaining.

Discussion

The present data indicate that MCT1 immunoreactivity in ASPS corresponds to the characteristic PAS-diastase-resistant cytoplasmic granules that undergo crystalliza-
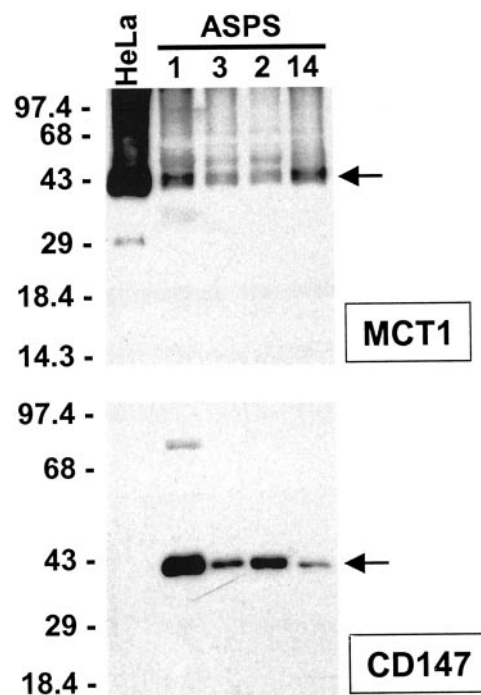
Figure 4. Western blot analysis of MCT1 and CD147 in ASPS tissues. Four ASPS cases from the present series were analyzed with the same antibodies used for IHC, along with HeLa human cervical carcinoma cells as a control. Equivalent amounts of protein were loaded in each lane. All four ASPS cases and HeLa cells show the expected 43-kd MCT1 band.[14] The four ASPSs, but not HeLa cells, show the expected 42-kd CD147 band.[14] The faint band migrating at ~86 kd may represent CD147 dimers in this case with especially strong expression. CD147 dimer formation has been previously reported.[28] In HeLa cells, MCT1 expression has been previously demonstrated,[29] but there are to our knowledge no previous studies of CD147 in this cell line.


Figure 3. Ultrastructural localization of MCT1 immunoreactivity in ASPS. Results of ultrastructural IHC of case ASPS-2 are illustrated. The MCT1 antibody resulted in deposition of gold particles on the cytoplasmic dense granules (original magnification, ×14,000). For comparison, the density of particle deposition shown here for MCT1 is greater than that previously demonstrated on normal mitochondria.[13]

tion to produce the pathognomic crystals of ASPS. Immunostaining with a polyclonal antibody to CD147 shows that the PAS-diastase-resistant cytoplasmic granules of ASPS are also immunoreactive for this protein, which is known to bind to MCT1 and facilitate its appropriate targeting to the cell membrane. These results are supported by ultrastructural IHC analyses using MCT1 antibody. Moreover, Western blot analysis confirmed that the two antibodies are binding to proteins of the respective expected molecular weight in ASPS tissues. Taken together, these results indicate that MCT1-CD147 complexes accumulate and possibly crystallize in the cytoplasm of ASPS cells. Our results do not exclude the possibility of additional proteins in the composition of the granules and crystals of ASPS. The pattern of cytoplasmic immunoreactivity observed in our ASPS cases was mostly granular or globular, with some polygonal forms, in contrast to the longer rhomboid-shaped appearance of fully developed crystals. We hypothesize that MCT1 and CD147 immunoreactivity may be reduced by complete crystallization, accounting for the stronger staining of the PAS-diastase-resistant dense granules.

It has been reported that crystals with the same or similar periodicity and structure have occasionally been observed in other human tumors and tissues,[15] most notably in the epithelioid smooth muscle cells of renal angiomyolipoma.[16] Indeed, we have studied a single case of renal angiomyolipoma that showed ASPS-type crystals by electron microscopy and found discrete cytoplasmic granular immunoreactivity for MCT1 in a pattern similar to the ASPS cases described above (M Ladanyi, CR Antonescu, unpublished results).

It is not clear whether this intracellular accumulation of MCT1-CD147 complexes in ASPS is because of overproduction or impaired trafficking to their normal destination at the cell membrane. Aberrant overproduction could hypothetically be related to the action of APSL-TFE3 in ASPS cells, but it is not known whether the promoters of *MCT1* or *CD147* contain TFE3-responsive elements that might be inappropriately activated by ASPL-TFE3. The *MCT1* promoter has not been isolated.[17] The *CD147* promoter sequence is available (GenBank no. AF042848)[18] and database analysis (MatInspector; Genomatix Software, Munich, Germany) identifies two potential TFE3 binding sites, CACGTG at −223 and CATGTG at −475 (analysis not shown), which would need to be validated as functional TFE3-binding sites by transactivation assays and related analyses.

Impaired trafficking could reflect an imbalance in the amount of MCT1 and CD147, which normally complex together in a 1:1 ratio,[14] or could be because of a deficiency in other, as yet uncharacterized, proteins necessary for the correct targeting of MCT1-CD147 complexes to the cell membrane. It should be noted that cell membrane immunostaining was heterogeneous in the present series, with all cases showing at least some MCT1 positivity whereas CD147 was more variable, with some cases completely lacking membrane immunoreactivity for this protein (Table 1).

The *MCT1* gene (*SLC16A1*) at 1p13-p12 encodes a ubiquitously expressed proton-linked transporter for monocarboxylates such as lactate and pyruvate.[17] Appropriate localization of MCT1 at the cell surface requires a direct interaction with CD147.[14] Expression of MCT1 in skeletal muscle is especially high in slow oxidative (type I) fibers where it is up-regulated in response to exercise, consistent with a role in lactic acid influx for oxidation as a respiratory fuel.[17] MCT1 is also prominent in other cells, including red blood cell membranes.[17]

The *CD147* gene at 19p13.3 encodes a ubiquitously expressed highly glycosylated transmembrane glycoprotein belonging to the immunoglobulin superfamily. It functions as an MCT-associated chaperone protein and as a cell surface inducer of matrix metalloproteinases.[19] It is identical or highly related to human M6 or EMMPRIN, mouse gp42 or basigin, rat OX-47 or CE-9, and avian HT7 or 5A11 or neurothelin.[20,21] As an inducer of extracellular matrix metalloproteinases, its forced overexpression in certain cancer cell lines has been shown to increase their tumorigenic potential.[22] Increased matrix degradation because of induction of matrix metalloproteinases by surface CD147 overexpression could also be relevant to the loss of central cohesion within nests of ASPS cells that produces its characteristic pseudoalveolar appearance.

CD147 is also of interest as a potential therapeutic target. ABX-CBL, a cytotoxic murine monoclonal antibody directed against CD147, has shown promise in a pilot study of patients with acute graft-*versus*-host disease, presumably because of its selective targeting of activated B and T cells that express more CD147 than resting lymphocytes.[23] The CD147 overexpression in ASPS, which includes in some cases prominent membranous expression, may make these tumors especially sensitive to CD147-targeted immunotherapy.

The histogenesis or differentiation lineage of ASPS has been one of the longest-running controversies in tumor histopathology.[3] A proposed origin from skeletal muscle precursor cells, based on reported immunoreactivity for certain muscle-associated proteins (most consistently, desmin) has generated considerable controversy.[24–27] Hopes that the cloning of the genes involved in the specific translocation in ASPS, the t(X;17)(p11.2;q25), might shed light on its histogenesis were dashed by the observation that, of the two translocation partners, *ASPL* and *TFE3*, neither shows a tissue-specific expression pattern. Likewise, it is difficult to draw any further insight into this issue from the finding that the granules and crystals of ASPS contain MCT1 and CD147. Although the expression of MCT1 is especially prominent in skeletal and cardiac muscle,[17] both proteins are expressed in a wide variety of tissues.

References

1. Lieberman PH, Brennan MF, Kimmel M, Erlandson RA, Garin-Chesa P, Flehinger BY: Alveolar soft-part sarcoma. A clinicopathologic study of half a century. Cancer 1989, 63:1–13
2. Enzinger FM, Weiss SW: Malignant soft tissue tumors of uncertain histogenesis. Soft Tissue Tumors. Edited by FM Enzinger, SW Weiss. St. Louis, Mosby, 1995, pp 1067–1093
3. Ordonez NG: Alveolar soft part sarcoma: a review and update. Adv Anat Pathol 1999, 6:125–139
4. Christopherson WM, Foote FW, Stewart FW: Alveolar soft-part sarcomas; structurally characteristic tumors of uncertain histogenesis. Cancer 1952, 5:100–111
5. Heimann P, Devalck C, Dubusscher C, Sariban E, Vamos E: Alveolar soft-part sarcoma: further evidence by FISH for the involvement of chromosome band 17q25. Genes Chromosom Cancer 1998, 23:194–197
6. Joyama S, Ueda T, Shimizu K, Kudawara I, Mano M, Funai H, Takemura K, Yoshikawa H: Chromosome rearrangement at 17q25 and Xp11.2 in alveolar soft-part sarcoma: a case report and review of the literature. Cancer 1999, 86:1246–1250
7. Ladanyi M, Lui MY, Antonescu CR, Krause-Boehm A, Meindl A, Argani P, Healey JH, Ueda T, Yoshikawa H, Meloni-Ehrig A, Sorensen PHB, Mertens F, Mandahl N, Van Den Berghe H, Sciot R, Dal Cin P, Bridge JA: The der(17)t(X;17)(p11;q25) of human alveolar soft part sarcoma fuses the TFE3 transcription factor gene to ASPL, a novel gene at 17q25. Oncogene 2001, 20:48–57
8. Shipkey FH, Lieberman PH, Foote FW, Stewart FW: Ultrastructure of alveolar soft part sarcoma. Cancer 1964, 17:821–830
9. Tucker JA: Crystal-deficient alveolar soft part sarcoma. Ultrastruct Pathol 1993, 17:279–286
10. Menesce LP, Eyden BP, Edmondson D, Harris M: Immunophenotype and ultrastructure of alveolar soft part sarcoma. J Submicrosc Cytol Pathol 1993, 25:377–387
11. Mukai M, Torikata C, Iri H: Alveolar soft part sarcoma: an electron microscopic study especially of uncrystallized granules using a tannic acid-containing fixative. Ultrastruct Pathol 1990, 14:41–50
12. Sciot R, Dal Cin P, De Vos R, Van Damme B, de Wever I, Van Den Berghe H, Desmet VJ: Alveolar soft-part sarcoma: evidence for its myogenic origin and for the involvement of 17q25. Histopathology 1993, 23:439–444
13. Brooks GA, Brown MA, Butz CE, Sicurello JP, Dubouchaud H: Cardiac and skeletal muscle mitochondria have a monocarboxylate transporter MCT1. J Appl Physiol 1999, 87:1713–1718
14. Kirk P, Wilson MC, Heddle C, Brown MH, Barclay AN, Halestrap AP: CD147 is tightly associated with lactate transporters MCT1 and MCT4 and facilitates their cell surface expression. EMBO J 2000, 19:3896–3904
15. Carstens PHB: Membrane-bound cytoplasmic crystals, similar to those in alveolar soft part sarcoma, in a human muscle spindle. Ultrastruct Pathol 1990, 14:423–428
16. Mukai M, Torikata C, Iri H, Tamai S, Sugiura H, Tanaka Y, Sakamoto M, Hirohashi S: Crystalloids in angiomyolipoma. 1. A previously unnoticed phenomenon of renal angiomyolipoma occurring at a high frequency. Am J Surg Pathol 1992, 16:1–10
17. Halestrap AP, Price NT: The proton-linked monocarboxylate transporter (MCT) family: structure, function and regulation. Biochem J 1999, 343:281–299
18. Guo H, Majmudar G, Jensen TC, Biswas C, Toole BP, Gordon MK: Characterization of the gene for human EMMPRIN, a tumor cell surface inducer of matrix metalloproteinases. Gene 1998, 220:99–108
19. Sun J, Hemler ME: Regulation of MMP-1 and MMP-2 production through CD147/extracellular matrix metalloproteinase inducer interactions. Cancer Res 2001, 61:2276–2281
20. Seulberger H, Unger CM, Risau W: HT7, neurothelin, basigin, gp42 and OX-47—many names for one developmentally regulated immuno-globulin-like surface glycoprotein on blood-brain barrier endothelium, epithelial tissue barriers and neurons. Neurosci Lett 1992, 140:93–97
21. Spring FA, Holmes CH, Simpson KL, Mawby WJ, Mattes MJ, Okubo Y, Parsons SF: The Oka blood group antigen is a marker for the M6 leukocyte activation antigen, the human homolog of OX-47 antigen, basigin and neurothelin, an immunoglobulin superfamily molecule that is widely expressed in human cells and tissues. Eur J Immunol 1997, 27:891–897
22. Zucker S, Hymowitz M, Rollo EE, Mann R, Conner CE, Cao J, Foda HD, Tompkins DC, Toole BP: Tumorigenic potential of extracellular matrix metalloproteinase inducer. Am J Pathol 2001, 158:1921–1928
23. Deeg HJ, Blazar BR, Bowell BJ, Long GD, Schuening F, Cunningham J, Rifkin RM, Abhyankar S, Briggs AD, Burt R, Lipani J, Roskos LK, White JM, Havrilla N, Schwab G, Heslop HE: Treatment of steroid-refractory acute graft-versus-host disease with anti-CD147 monoclonal antibody ABX-CBL. Blood 2001, 98:2052–2058
24. Rosai J, Dias P, Parham DM, Shapiro DN, Houghton P: MyoD1 protein expression in alveolar soft part sarcoma as confirmatory evidence of its skeletal muscle nature. Am J Surg Pathol 1991, 15:974–981
25. Tallini G, Parham DM, Dias P, Cordon-Cardo C, Houghton PJ, Rosai J: Myogenic regulatory protein expression in adult soft tissue sarcomas. A sensitive and specific marker of skeletal muscle differentiation. Am J Pathol 1994, 144:693–701
26. Gomez JA, Amin MB, Ro JY, Linden MD, Lee MW, Zarbo RJ: Immunohistochemical profile of myogenin and MyoD1 does not support skeletal muscle lineage in alveolar soft part sarcoma. Arch Pathol Lab Med 1999, 123:503–507
27. Wang NP, Bacchi CE, Jiang JJ, McNutt MA, Gown AM: Does alveolar soft-part sarcoma exhibit skeletal muscle differentiation? An immunocytochemical and biochemical study of myogenic regulatory protein expression. Mod Pathol 1996, 9:496–506
28. Fadool JM, Linser PJ: Evidence for the formation of multimeric forms of the 5A11/HT7 antigen. Biochem Biophys Res Commun 1996, 229:280–286
29. Lin RY, Vera JC, Chaganti RS, Golde DW: Human monocarboxylate transporter 2 (MCT2) is a high affinity pyruvate transporter. J Biol Chem 1998, 273:28959–28965